ASSESSMENT OF PROBABILISTIC FLOOD FORECASTING USING ENSEMBLE NWP RAINFALL WITH 30HR FORECAST TIME DURING TYPHOON EVENTS

Wansik YU [1], Eiichi NAKAKITA [2], and Kosei YAMAGUCHI [3]

[1]Student Member of JSCE, PhD. Student, Department of Civil and Earth Resources Engineering, Kyoto University (Gokasho, Uji, Kyoto 611-0011, Japan)
[2]Member of JSCE, Professor, DPRI, Kyoto University (Gokasho, Uji, Kyoto 611-0011, Japan)
[3] Member of JSCE, Assistant Professor, DPRI, Kyoto University (Gokasho, Uji, Kyoto 611-0011, Japan)

On early September, 2011, Typhoon Talas caused local heavy rainfalls over the Kinki, Chugoku, Shikoku and Tokai regions in Japan. The operational meso-scale model of the JMA generally predicted the typhoon track well in the early period. However, the rainfall intensity was weaker than expected, and the movement was also faster when the lead time was longer. This study aimed to assess whether the latest ensemble NWP outputs with 30hr forecast time and 2km horizontal resolution from MRI can produce suitable rainfall predictions or not, and to assess the hydrological applicability of ensemble flood forecasts driven by the latest ensemble NWP rainfall. As a result, ensemble rainfall prediction produced more suitable results compared with a deterministic control run in terms of QPF. Ensemble flood forecasting driven by ensemble rainfall forecasts could also produce comparable results in comparisons of observed data, although the maximum peak discharge value was underestimated.

Key Words: *Typhoon Talas, Ensemble NWP rainfall, Probabilistic Flood Forecasting, Error Propagation*

1. INTRODUCTION

In early September, 2011, local heavy rainfalls due to season's 12th typhoon, "Talas" caused large flooding and enormous landslide disasters over the Kinki, Chugoku, Shikoku, and Tokai regions in Japan. It also caused unprecedented human damages, resulting in 78 dead and 16 missing persons. Talas moved very slowly and had a huge gale diameter throughout its life. The total amount of the precipitation exceeded 1,000mm in the Kii Peninsula.

In these types of extreme events, it is essential to be able to provide as much advance warning as possible. This advance warning requires both quantitative precipitation forecasting (QPF) and quantitative flood forecasting (QFF). Numerical Weather Prediction (NWP) models are now becoming standard for short-range (1~2days) forecasts. The Meso-Scale Model (MSM) of Japan Meteorological Agency (JMA) is now run operationally with a horizontal resolution of 5km. During the Typhoon Talas event, the MSM generally predicted the typhoon track well in the early period. However, the predicted rainfall intensity was weaker than the observed radar rainfall, and the movement was also faster, as the lead time was longer. As a result, the rainfall forecast pattern moved to the north-eastern part of the Kii peninsula quickly. One of the methods to overcome the forecast failure of deterministic predictions is to use ensemble outputs of NWP models. In cases of extreme events like typhoon Talas, the forecast accuracy is generally low. Therefore ensemble forecast systems are needed, and it is believed that ensemble prediction systems exhibit greater forecast skill than a single NWP model.[1)] Another method for an improvement in accuracy can be achieved by increasing in the resolution of NWP models. In Japan, the JMA's operational one-week ensemble prediction has been developed to support typhoon track forecast and to provide probabilistic information with a horizontal resolution of 60km and 51 Ensemble members. However, there is a limitation to use one-week ensemble prediction in respect of hydrological

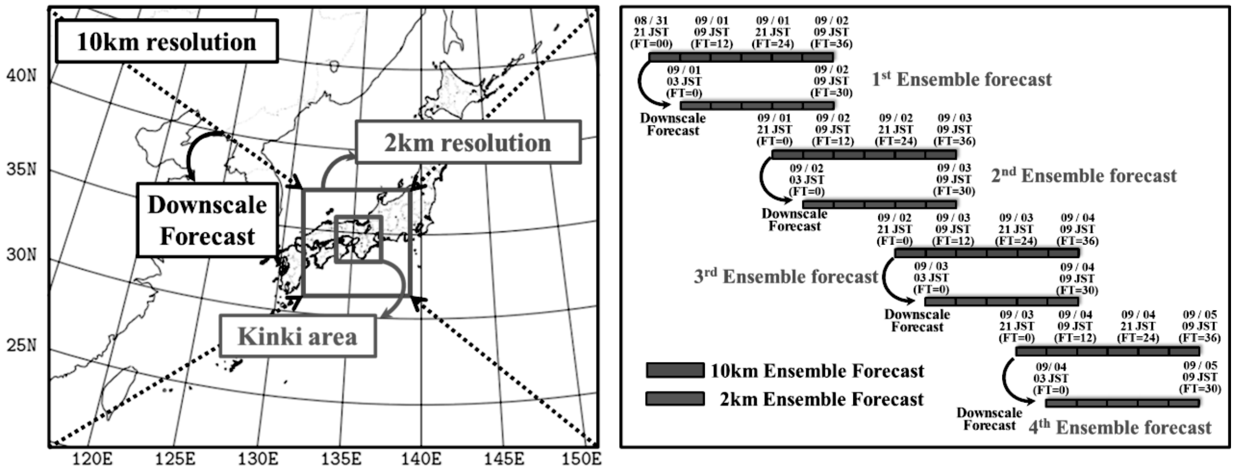

Fig. 1 (a) Forecast domains of 10km and 2km horizontal resolution; the rectangle inside 2km domain denotes the verification area. (b) A schematic of four sets of forecast runs (blue and red boxes denote the 10km and 2km horizontal resolutions, respectively.) Forecast period of 2km horizontal resolution: 1st forecast (2011/09/01 03:00 ~ 09/02 09:00), 2nd forecast (2011/09/02 03:00 ~ 09/03 09:00), 3rd forecast (2011/09/03 03:00 ~ 09/04 09:00), 4th forecast (2011/09/04 03:00 ~ 09/05 09:00), and each forecast period of 2km resolution is overlapped with 6 hours.

applications because one-week ensemble prediction has a coarse spatial resolution. With consideration for high-resolution and ensemble forecasts, the latest ensemble NWP forecast with 30hr forecast time and 2km horizontal resolution has been generated by the Meteorological Research Institute (MRI) of the JMA, and is still in research for an improvement in terms of the forecast accuracy. This ensemble NWP forecast is not yet operational, and it is expected that this ensemble NWP prediction can improve the forecast skill more than operational deterministic rainfall forecasts.

In the context of flood management, it is important to integrate NWP model output and flood forecasts. It is possible to incorporate NWP model outputs directly into flood forecasting systems to obtain an extended lead time. [2] However, direct application of deterministic NWP model output can propagate uncertainties into the hydrologic domain. For these reasons, the development of ensemble hydrological applications started in the late 1990s and is a field of ongoing research.[3), 4)] Ensemble flood forecasting provides additional information to the deterministic flood forecast in the short forecast range, and provides a signal in terms of pre-warning and exceedance probabilities for threshold values (e.g. critical discharge, levels causing inundation, and so on).

In this study, we aim to overcome an insufficiency of the deterministic flood forecast using ensemble outputs with 30hr forecast time and 2km high-resolution, it is not purpose to use the information of the ensemble mean value. Therefore, we assess the latest ensemble NWP outputs with 30hr forecast time and 2km horizontal resolution from MRI whether they can produce suitable rainfall predictions or not during the Typhoon Talas event, and we also assess the performance of ensemble flood forecasting for hydrological applications based on the latest ensemble NWP forecast with 30hr forecast time and 2km horizontal resolution. In this study, it is important that the ensemble flood forecast with 30hr forecast time and 2km high-resolution has not been carried out in previous researches of the flood forecast field. Finally, we assess the error propagation from ensemble NWP rainfall to streamflow as a function of spatial scale in the Shingu river basin.

2. METHODOLOGY

(1) Short-range ensemble rainfall forecast

We used two ensemble systems with 10km and 2km horizontal resolution. The latest forecast model was developed and implemented by MRI of JMA for rainfall forecast using nonhydrostatic model.[5)] Whereas the 10km resolution forecast adopted the cloud microphysical process and Kain-Fritsch convective scheme, the 2km resolution forecast did not have to use a convective scheme because of its cloud resolving resolutions. The ensemble system consists of 10 perturbed and one unperturbed (or control run). One forecast, the “control run,” is forecast with a non-perturbed analysis and is similar to the MSM of JMA from the viewpoints of initial and lateral boundary conditions. The 10 perturbed forecasts of ensemble system result from a perturbation technique based on a mathematical method called the local ensemble transform Kalman filter (LETKF) method.[6)] Initial conditions of the 2km ensemble forecast were given by the 6hr forecast time of the 10km ensemble forecast results. The domain of the two ensemble systems with 10km and 2km horizontal resolution are illustrated in **Fig.**

1(a). The 10km and the 2km resolutions had a domain of 361×289 grid points and 350×350 grid, respectively. At first, a meso ensemble prediction with a horizontal resolution of 10km was performed up to 36hr forecast time at 9pm JST, and its downscale prediction with a horizontal resolution of 2km was performed up to 30hr forecast at 3am JST. This process is continued during the Typhoon Talas event. Therefore, we constructed the 4 sets of ensemble prediction outputs with 10km and 2km horizontal resolution (**Fig. 1(b)**), and we introduce the results of ensemble prediction with 2km horizontal resolution due to the viewpoints of high-resolution and better predictability of weather phenomena in this study.

(2) Distributed grid-based hydrologic model

We used the grid-based one-dimensional kinematic wave method for subsurface and surface flow simulation, which was enhanced by Tachikawa et al.[7] In this model, the drainage network is represented by sets of hillslope and channel elements from the digital elevation model. Each element is represented by a rectangle formed by two adjacent nodes of grid cells. The rainfall over all hillslope elements flows one-dimensionally into the river nodes and then routes to the catchment outlet. The rainfall-runoff transformation is based on the assumption that each hillslope element is covered with a permeable soil layer. This soil layer consists of a capillary layer and a non-capillary layer. In these conceptual soil layers, slow and quick flow are simulated as unsaturated and saturated flow, respectively, and surface flow occurs if water depth, h (m) exceeds soil water capacity.

$$q=\begin{cases} v_c d_c (h/d_c)^{\beta}, & 0 \le h \le d_c \\ v_c d_c + v_a (h-d_c), & d_c \le h \le d_s \\ v_c d_c + v_a (h-d_c) + \alpha (h-d_s)^m, & d_s \le h \end{cases} \qquad (1)$$

The discharge per unit width q [m^2/s] is calculated by Eq. (1), combined with the continuity equation, where $v_c = k_c i$, $v_a = k_a i$, $k_c = k_a / \beta$, m=5/3, k_c and k_a are the hydraulic conductivity of the capillary soil layer and non-capillary soil layer, respectively. n is the roughness coefficient, and d_c and d_s are soil depth in the capillary and non-capillary pore, respectively

3. RESULTS AND DISCUSSION

(1) Study area

Typhoon Talas caused enormous flooding and landslide disasters in the Shingu River Basin, and many roads were damaged as well as electricity, communication lines and water supply. Therefore, in this study, we selected the Shingu River Basin as the study area to assess the flood forecast applicability utilizing the ensemble NWP rainfall. Shingu River Basin is located in the Kii peninsula of the Kinki region, Japan and covers an area of 2,360 km^2 (**Fig. 2**). The topography of the basin is characterized by a mountainous upstream in the north and a flatter plain in the south. The elevation in the basin ranges from 11 to 1892 m, with an average of about 644 m. The five dams Futatsuno, Kazeya, Komori, Nanairo, and Ikehara are located upstream.

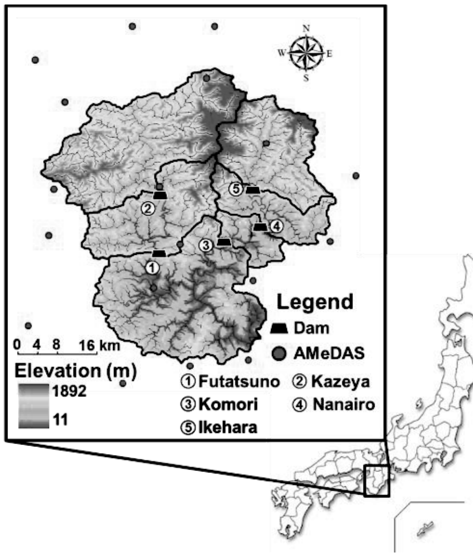

Fig. 2 Study area within Kii peninsula in Japan.

(2) Ensemble NWP rainfall

a) The temporal verification

For the purpose of temporal verification of QPF with ensemble NWP rainfall during the Talas event, we compared the areal rainfall intensity between the Automated Meteorological Data Acquisition System (AMeDAS) and ensemble prediction over the Shingu River Basin (2,360 km^2, **Fig. 2**) in the form of box plots[8]. For comparison, the observed rainfall of AMeDAS (18 stations, 10min step) is interpolated using the Thiessen polygon spatial distribution method. In the 1st and 2nd forecast period of **Fig. 3(a)**, the control run and ensemble forecast produced a suitable areal rainfall compared with the AMeDAS rainfall, but as shown in the 3rd forecast result, on which focused in this study, the control run forecast was well not matched and did not produce the rainfall intensity because the spatial pattern of raincells moved to the north-eastern part of Kii peninsula quickly by that the MSM failed to correctly forecast, as mentioned in the introduction section. On the other hand, the upper range of the ensemble forecast was able to produce considerable rainfall intensity, and the amounts of maximum rainfall intensity are also similar to AMeDAS rainfall. In 4th forecast period, the reason why

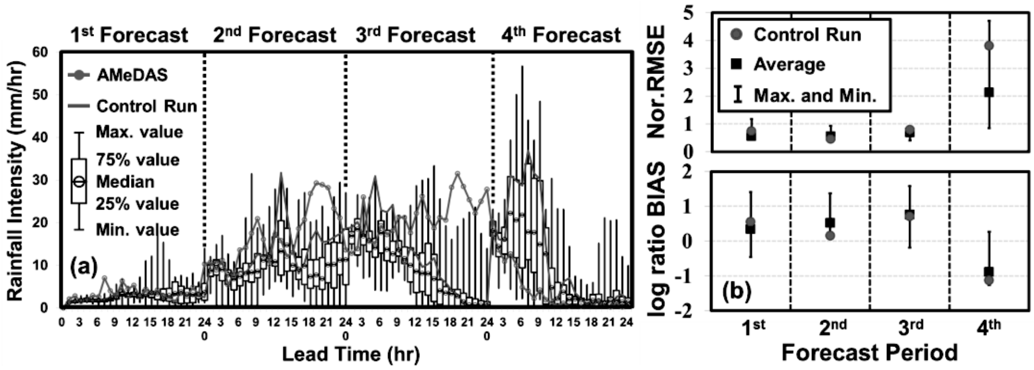

Fig. 3 (a) Ensemble areal rainfall forecast over the Shingu River Basin in the form of box plots plotted from 0 to 24hr forecast time, excluding overlapped forecast time (from 25 to 30hr) for the overall comparison for the Typhoon Talas. (b) Verification results of areal rainfall with normalized RMSE and log ratio bias for Typhoon Talas. Red circles and black squares mean the indexes of the control run and the mean value of ensemble forecast, respectively. The lower and upper bounds of the black lines correspond to the minimum and maximum values, respectively.

rainfall intensities are overestimated can be explained by the fact that the last spatial rainfall pattern of the 3rd forecast moved to the north-eastern part of the Kii peninsula; however, it started the forecast again from the Kii peninsula in the 4th forecast. For this reason, rainfall intensities were very high in the 4th forecast period compared with AMeDAS. To evaluate the accuracy of the control run and ensemble forecast in terms of areal rainfall intensity, we calculated two error indexes (**Fig. 3(b)**). The first is the normalized root mean square error (RMSE), which is normalized by the mean value of the observations during the each forecast period (30hr). The second is the log ratio bias, which a relative error and provides information about the total amount of rainfall. A log ratio bias value of zero indicates a perfect forecast; positive and negative values indicate underestimated and overestimated forecasts, respectively. In the index of normalized RMSE, the control run and ensemble mean have similar values from 1st to 3rd forecast period, but the best index of the ensemble forecast could provide good value as compared with the deterministic control run. In the 4th forecast period, as mentioned above, the index of the control run and ensemble spread is relatively large, but the best index of the ensemble is estimated at 0.84 (the control run is 3.81). In the index of the log ratio bias, the best index of ensemble spread was close to zero value (perfect forecast), whereas the control run forecast was underestimated for the 1st, 2nd, and 3rd forecasts, and overestimated for the 4th forecast period.

b) The spatial verification

The ensemble NWP rainfall forecast in this study have been verified spatially against the Ministry of Land, Infrastructure, Transport and Tourism (MLIT) composite radar data, because their high spatial-temporal resolution is suitable to capture the spatial variability of rainfall. The ensemble forecasts were expressed as probabilities of exceeding selected rainfall thresholds (0.1 mm/h). A contingency table can be constructed by a spatial comparison of yes/no forecasts and yes/no observed rainfall, given the rainfall threshold. In this study, we used critical success index (CSI, also called the "threat score"), probability of detection (POD, also

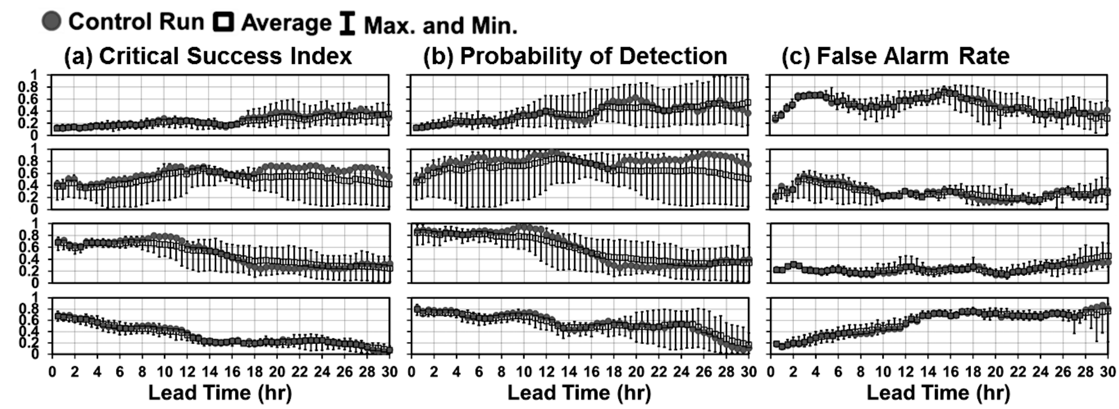

Fig. 4 (a) CSI; its range is 0 to 1, with a value of 1 indicating a perfect forecast. It takes into account both false alarms and missed events. (b) POD; it is the ratio of the number of correct forecasts over the total number of times the rainfall observed. Its range is 0 to 1, with a value of 1 indicating a perfect forecast. (c) FAR; it is the ratio of the number of false alarm over the total number of times the rainfall forecast. Its range is 0 to 1, with a value of 1 indicating a poor forecast. The value of each row shows the index of from 1st to 4th forecast outputs with lead time.

called “hit rate”), and false alarm rate (FAR) for spatial qualitative verification of ensemble forecast outputs in the Kinki region (**Fig. 1(a)**). CSI, POD and FAR are given by [8]:

$$CSI = \frac{hits}{hits + misses + false\,alrms} \quad (2)$$

$$POD = \frac{hits}{hits + misses} \quad (3) \qquad FAR = \frac{false\,alrms}{hits + false\,alrms} \quad (4)$$

Where hits are the number of correct forecasts over the threshold (i.e. rainfall is forecast and also observed), and misses are the number of times rainfall is not forecast, but is observed. False alarms are the number of times rainfall is forecast but is not observed. **Fig. 4** shows the results of CSI, POD, and FAR in a comparison of radar data and ensemble forecasts in the 1st, 2nd, 3rd, and 4th forecast period. In the 3rd forecast period, on which we focused in this study, the CSI and the POD decreased and the FAR increased as lead time increased. However, the values of the ensemble forecast could maintain higher forecast accuracy compared to the control run forecast. It showed that ensemble forecasts have an advantage in terms of spatial accuracy, although lower value of ensemble forecasts exists in each forecast period as lead time increases.

(3) Probabilistic flood forecast

We considered two dams located in the Shingu River Basin: Futatsuno and Nanairo (Nos. 1 and 4 of **Fig. 2**), for an assessment of the probabilistic flood forecast driven by ensemble NWP rainfall in this study. Two other dams, Kazeya and Ikehara (Nos. 2 and 5 of **Fig. 2**), are in the upstream of the Futatsuno and Nanairo dam basins, respectively. The outflow record from each upstream dam was considered input data in a distributed hydrologic model. First, we conducted the parameter optimization of the hydrologic model using MLIT composite radar data and Shuffled Complex Evolution (SCE) global optimization method.[9] Next, we used the simulated discharge from the observed radar rainfall as the initial condition for the ensemble flood forecast driven by the ensemble NWP rainfall. **Fig. 5** shows the results of the 30hr ensemble flood forecast over the Futatsuno and Nanairo dams for Typhoon Talas. As shown in **Figs. 5(a) and (b)**, the 1st and 2nd forecast (rising limbs) of both the control run and ensemble forecast produced a suitable discharge, but were lower than the true value from 20 to 30hr lead times of the 2nd forecast period over the Futatsuno Dam Basin, caused by the underestimation of the rainfall forecast. In the 3rd forecast period of peak discharge, on which we focused in this study, the control run forecast was typically lower than the observed discharge, caused by its shift from the correct spatial position. The majority of ensemble members were also lower than the observed discharge, but a few ensemble members exceeded the control run forecast, and were close to the observed discharge in both the Futatsuno and Nanairo dam basins. In the 4th forecast period (falling limb), both the control run and ensemble forecast were overestimated because the over-estimation in rainfall forecast (4th forecast of **Fig.5**) triggered a runoff over-estimation. The scatter plots of Futatsuno and Nanairo dam basin show that the ensemble forecasts had better results than the control run forecast in terms of the coefficient of determination (also called the “R-squared”) which is used to describe how well a regression line fits a set of observed data (**Fig. 5**). In these results, the ensemble flood forecasts provided additional information (e.g. the indication of the possibility of an extreme event) that were not present in the deterministic forecast, and this additional information could be used for real-time flood forecast, dam inflow forecast, and dam release support. How this information should put into decision support, however, needs to be examined in more detail using a number of case studies to assess the performance of the probabilistic forecasts.

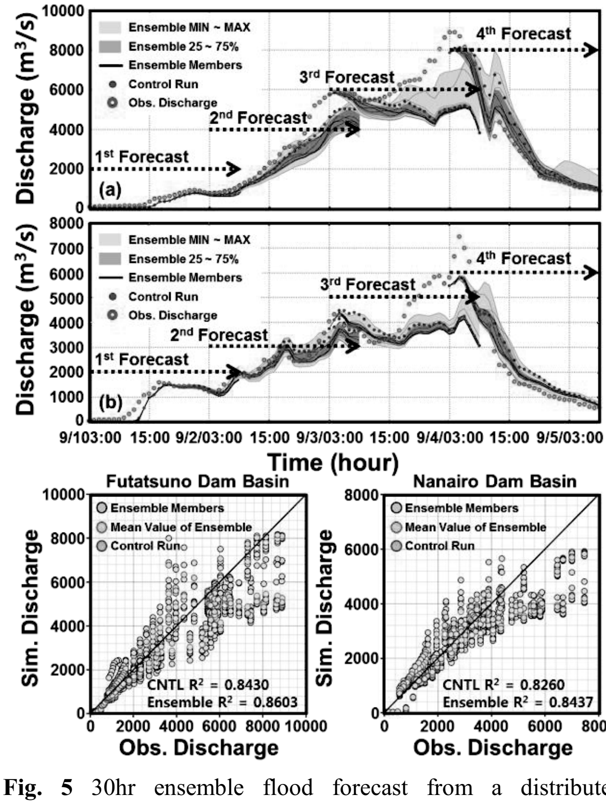

Fig. 5 30hr ensemble flood forecast from a distributed hydrologic model for Typhoon Talas: (a) Futatsuno Dam Basin (356.1km2) excluding Kazeya Dam Basin, and its scatter plot (b) Nanairo Dam Basin (182.1km2) excluding Ikehara Dam Basin, and its scatter plot.

(4) Error propagation with spatial scale

Rainfall forecasting errors arise because uncertainty exists in forecast timing, location, and magnitude in the rainfall field, and flood forecast skill critically depends on the spatial accuracy of the rainfall field. Despite its importance, error propagation from ensemble-based NWP rainfall to distributed flood forecast has not been addressed properly in terms of a quantitative point of view. In this section, we assessed the error propagation from ensemble NWP rainfall to flood forecast with sub-basins of Shingu River Basin. We used the index of root mean square error, each specific discharge (discharge/basin area) of outlets and the coefficient of determination to capture and confirm the relationship of error propagation as a function of spatial scale. **Fig. 6** presents the variation of RMSE based on the specific discharge with the basin area for each forecast period. In the 1st and 2nd forecasts (rising limbs), as the basin area became larger, it showed a little falling tendency, but could not find the significant effect of error propagation. In the 3rd and 4th forecast periods (peak discharge and falling limb), the index of RMSE value decreased with basin scale, implying a much higher error propagation for the small basins. This result indicates that sensitivity of the basins to differences in rainfall input increases as basin scale decreases and caused a much higher uncertainty in ensemble flood forecast. It also implies that differences in error propagation are caused by the spatial variation of rainfall amount.

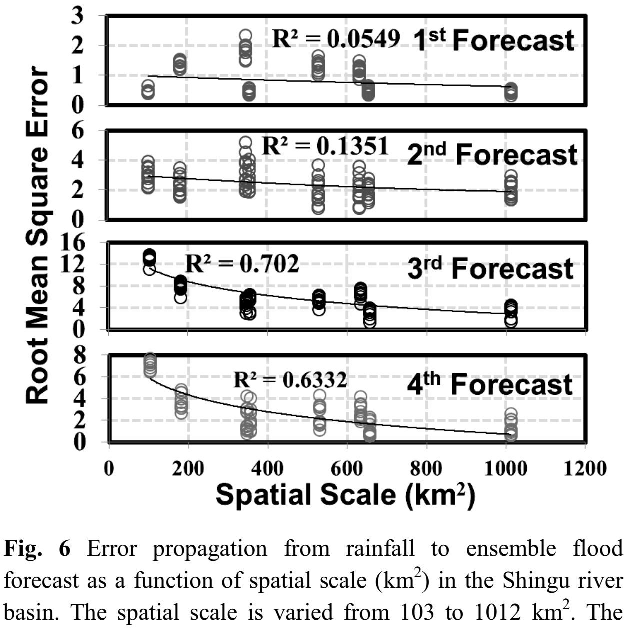

Fig. 6 Error propagation from rainfall to ensemble flood forecast as a function of spatial scale (km^2) in the Shingu river basin. The spatial scale is varied from 103 to 1012 km^2. The result is shown in terms of the RMSE. Note that RMSE are evaluated for each sub-basin based on the specific discharge (discharge/basin area).

4. CONCLUSION

Flood forecast driven by ensemble-based NWP rainfall was carried out in this study to assess the hydrological applicability during the Typhoon Talas event. It can be concluded from the study that ensemble NWP rainfall produced better results as compared with deterministic control run in terms of QPF, and the study showed that the ensemble flood forecasts provide more suitable results and additional information that is not present in the deterministic forecast, although peak discharge value was underestimated. In further research, through a number of case studies, ensemble NWP rainfall data could be used in hydrological applications such as real-time flood forecasting and dam operation.

ACKNOWLEDGMENT: This study was partly supported by the sub-project of the field 3 on Next Generation Supercomputer Project, 'Prediction of heavy rainfalls by a cloud-resolving NWP system', and was based on data from J-POWER CO. Ltd. We are grateful for their support.

REFERENCES

1) Lan Cuo, Pagano, T.C. and Wang, Q.J., A review of quantitative precipitation forecasts and their use in short-to medium-range streamflow forecasting, *Journal of Hydrometeorology*, Vol.12, pp.713-728, 2011
2) Xuan, Y., Cluckie, I. D. and Wang, Y., Uncertainty analysis of hydrological ensemble forecasts in a distributed model utilising short-range rainfall prediction, *Hydrol. Earth Syst. Sci.*, Vol.13, pp.293-303, 2009.
3) De Roo, A., Gouweleeuw, B., Thielen, J., et al., Development of a European Flood Forecasting System, *Intl. J. River Basin Management*, Vol. 1, No. 1, pp. 49-59, 2003.
4) Gouweleeuw, B., Thielen, J., Franchello, G., De Roo, A. and Buizza, R., Flood forecasting using medium-range probabilistic weather prediction, *Hydrol. Earth Syst. Sci.*, Vol.9, No.4, pp.365-380, 2005.
5) Saito, K., Ishida J., Aranami K., Hara T., Segawa T., Narita M., and Honda Y., Nonhydrostatic atmospheric models and operational development at JMA, *J. Meteor. Soc. Japan*, 85B, pp.271–304, 2007
6) Miyoshi, T. NHM-LETKF. *Tech. Rep*. MRI 62, 159-163, 2010.
7) Tachikawa, Y., Nagatani. G. and Takara, K., Development of stage discharge relationship equation incorporating saturated unsaturated flow mechanism, *Ann. J. Hydraul. Eng, JSCE* Vol.48, pp.7–12, 2004 (in Japanese)
8) Wilks,D.S., Statistical methods in the atmospheric sciences, Academic Press, London, UK, 2006.
9) Duan, Q., Sorooshian, S. and Gupta, V.K., Optimal use of the SCE-UA global optimization method for calibrating watershed models, *J. Hydrol.*, Vol.158, pp.265-284, 1994.

(Received April 4, 2013)